

# The AMS RICH PMTs calibration procedure

Diego Casadei<sup>1</sup>, Andrea Contin<sup>2</sup>

Dipartimento di Fisica, Università di Bologna, via Irnerio 46, I-40126 Bologna, Italy

August 24, 2001

## ABSTRACT

The AMS-02 RICH will have 11840 square pixels  $9 \times 9 \text{ mm}^2$ . Hamamatsu R7600-00-M16 photomultipliers ( $4 \times 4$  pixels) will be used for the photon counting. The important features of these devices are the pixel gain, single photoelectron resolution, and relative efficiency. The calibration procedure of 60 phototubes and few selection rules for the final detector are shown.

*Subject headings:* AMS-RICH: PMT gain, single photoelectron resolution, relative efficiency; PMT selection.

## 1. Introduction

The AMS-02 detector has a proximity focusing RICH sub-detector in place of the threshold Čerenkov counter of AMS-01 (see figure 1).

A 2 cm thick aerogel layer is used as Čerenkov radiator, and the light cones will expand for about 50 cm before reaching the pixels plane, parallel to the radiator layer. A conical mirror is used to gain acceptance, and the pixel plane has a square hole in front of the electromagnetic calorimeter (figure 2).

The total pixel number is 11840, and their size is  $9 \times 9 \text{ mm}^2$ . Hamamatsu R7600-00-M16 photomultipliers (PMT) are used for the photon counting. These 740 PMTs have  $4 \times 4$  pixels and are operated at  $-(750 \div 900) \text{ V}$ .

A set of 60 PMTs was tested in Bologna INFN laboratories and in Grenoble ISN laboratories, using two different read-out schemes.

## 2. The PMT test

In order to measure the gain and the single photoelectron resolution of every pixel, few (3 or 4) runs per PMT were done at different voltages, using a short-pulse LED emitting few photons per pulse.

Every run gives a “single photoelectron spec-

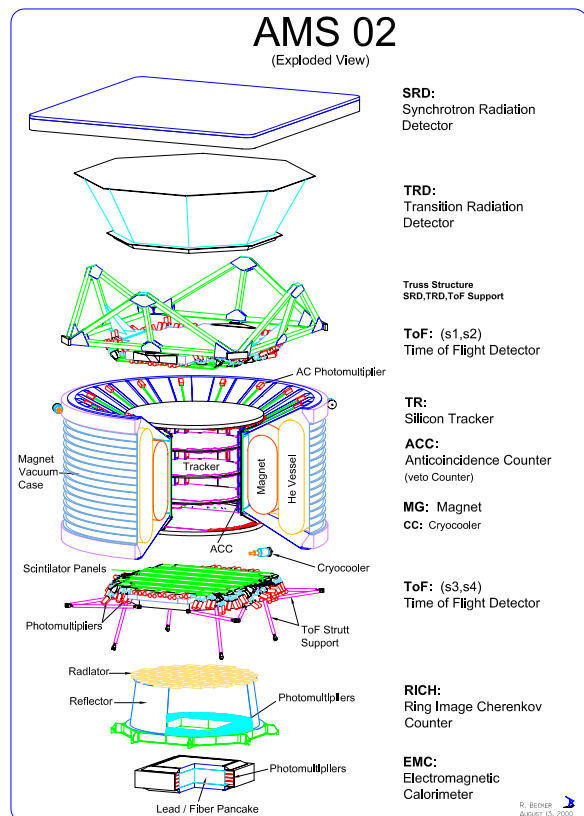
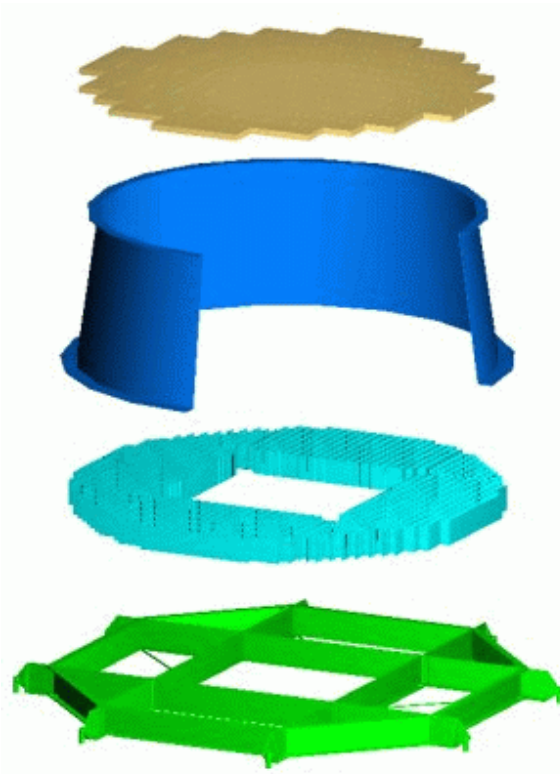


Figure 1. The AMS-02 detector.

<sup>1</sup>Diego.Casadei@bo.infn.it

<sup>2</sup>Andrea.Contin@bo.infn.it



**Figure 2.** The AMS-02 RICH detector.

trum”, i.e. a Poissonian charge distribution with a very low mean photoelectron number (figure 3). Such a spectrum has a recognizable “zero-peak” (the ADC pedestal) and “one-peak” (the single photoelectron signals distribution).

### 2.1. Gain

By definition, the distance between the zero- and one- peaks, divided by the electron charge, is the PMT *gain* at the given tension.

If we consider two Gaussian peaks with mean  $\mu_i$  and standard deviation  $\sigma_i$ , the gain  $G$  is the number:

$$G = \frac{(\mu_1 - \mu_0)Q_{\text{ADC}}}{e} \quad (1)$$

where  $Q_{\text{ADC}}$  is the charge per ADC count and  $e$  is the electron charge, while the uncertainty  $\Delta G$  is computed using the errors on  $\mu_i$  given by the fitting routine and the error on  $Q_{\text{ADC}}$ .

The latter was considered negligible, even if neglecting the uncertainty on  $Q_{\text{ADC}}$  means underestimating  $\Delta G$  of roughly 10% with the Bologna electronics

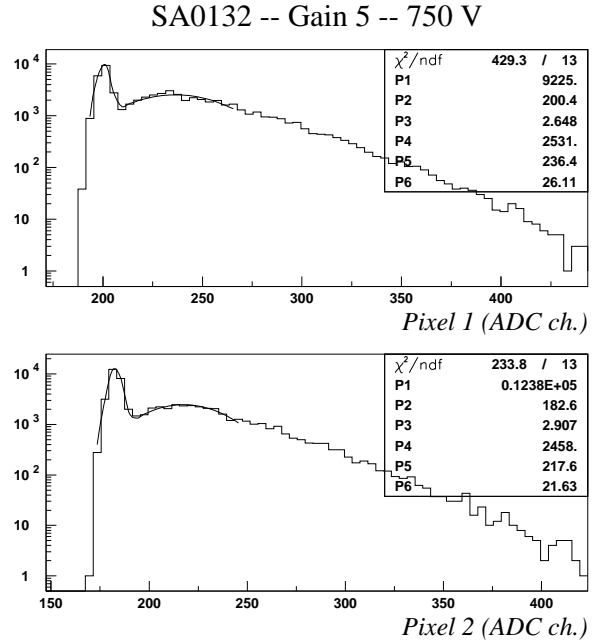


**Figure 3.** Two single photoelectron spectra.

( $\Delta Q_{\text{ADC}}/Q_{\text{ADC}} \approx 1.5\%$ ) and 50% with the Grenoble ADC chip ( $(\Delta Q_{\text{ADC}}/Q_{\text{ADC}})_{\text{eff}} \approx 5\%$ ).

The tension dependence of the gain is easily found by using a linear fit in a log-log scale:

$$\log_{10} G = P_1 + P_2 \log_{10} V \quad (2)$$

where  $P_i$  are the fit parameters and  $V$  is the absolute value of the operating voltage (see figure 4).

### 2.2. Single photoelectron resolution

The *single photoelectron resolution*  $\delta$  is the ratio between the standard deviation of the Gaussian one-peak, and its distance from the zero-peak:

$$\delta = \frac{\sigma_1}{\mu_1 - \mu_0} \quad (3)$$

(there is no need for  $Q_{\text{ADC}}$  here), and its error is computed using the fit uncertainties on  $\sigma_1$  and  $\mu_i$ . The smaller is  $\delta$ , the better is the photon counting.

### 2.3. Pixel efficiency

The absolute pixel efficiency cannot be measured with the devices available in Bologna and Grenoble, but the relative efficiency with respect to all other pixels of the same PMT can be evaluated looking at the

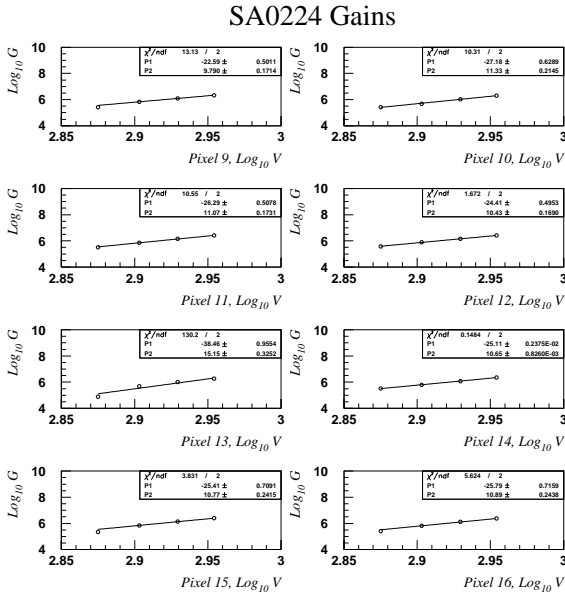


**Figure 4.** Linear fit of the gain to voltage log-log dependence.

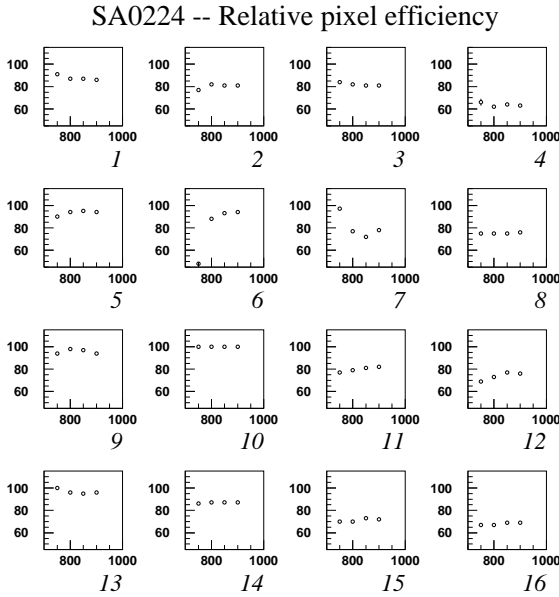


**Figure 5.** The relative pixel efficiency is almost insensitive to the HV settings.

normalization factors of the Gaussian fit of the one-peak (assuming that the same number of events is recorded in each run. See figure 5).

This is not comparable with the Hamamatsu data:

```
HV 1 2 3 4 5 6 7 8 9 10 11 12 GND
    360 360 360 150 150 150 150 150 150 150 150 180 360
    2.4:2.4:2.4: 1 : 1 : 1 : 1 : 1 : 1 : 1 : 1 : 1 : 1 : 1.2:2.4
```

**Figure 6.** First row: dynodes. Second row: resistors in  $k\Omega$ . Third row: repartition factors.

they measure the anodes current output when uniformly illuminating the pixels, i.e. what they quote as “Anode Uniformity” is the relative efficiency times the pixel gain.

A similar but different pixel efficiency definition was adopted to compare the pixels of all the PMTs, as described in §5.3.

### 3. PMT test in Bologna

A set of 80 PMTs was tested in Bologna, taking single photoelectron spectra at 3 different tensions.

Each PMT was put in a black box and connected to  $-900$  V for at least 15 minutes before the first test, in order to allow for decreasing of the PMT window photoluminescence induced by the environmental light.

Each PMT required roughly 1 hour to be tested. Three data sets of  $10^4$  events were taken, with  $-900$  V,  $-850$  V and  $-800$  V. For low gain PMTs the sequence was:  $-900$  V,  $-850$  V,  $-950$  V (always  $10^4$  events per run).

The voltage divider was always “hot” (no night turn off) and connected to some PMT, with the exception of the minute needed to change PMT. It was turned off during week ends and turned on for at least one hour before the next test. No significant change is noted after 18 hours (from 17:00 to 09:00) of continuous PMT operating.

#### 3.1. Setup

The voltage divider was from Hamamatsu (figure 6). The signals coming from the divider were read using LEMO  $50 \Omega$  cables. Even though the impedance is not exactly the same, the signals are good enough to take charge measurements.

The PMT was illuminated by a red LED driven at 60 Hz by a CAEN module (model C529), with roughly a 20 V amplitude pulse of 5 ns width. An opaque 2 mm thick plexyglass layer is used to diffuse light in a uniform manner (no difference is seen when rotating the PMT).

The anode signals are sent to a linear ADC (CAEN

model C205A) and digitized using the 0.033 pC/count scale. The relative uncertainty on the ADC conversion scale is 1.5%, but was neglected.

#### 4. PMT test in Grenoble

A subset of 60 PMTs was tested in Grenoble, taking single photoelectron spectra at 4 different tensions:  $-750$  V,  $-800$  V,  $-850$  V, and  $-900$  V.

##### 4.1. Setup

Each PMT required about 4 minutes to be tested. The LED was driven at roughly 2 kHz, and its light was carried on by light fibers to the PMT pixels. Every run is a set of 63'000 events. The PMTs were read by the RICH front-end chips and a custom board controlled by LabView.

The voltage divider was different from that used in Bologna, and was chosen due to its better linearity. The total impedance was 80 M $\Omega$  and the repartition was 2.4 : 2.4 : 1 : 1 : 1 : 1 : 1 : 1 : 1 : 1.2 : 2.4 : 2.4.

The anode signals are read by a 16 channels Analog Devices AD7476ART ADC chip situated on the flat cable coming out from the divider. Only one of the two gain scales of this 12 bits ADC was used, the “5 $\times$ ” scale (0.0037 pC/count, 5% uncertainty).

Channels 6 and 7 had problems: it seems that they had a positive offset, left-shifting the ADC distributions (anodes give negative signals) until truncation occurs. This offset is present, but not critical, also in “Gain 1” scale, that was used for those two channels only.

The resulting histograms were rebinned from 4096 to 1024 channels (not for pixels 6 and 7), in order to compensate for the great fluctuations between adjacent bins. Hence the effective resolution of the charge measurement is 10 bits, with 0.0146 pC/count. In addition, the resulting uncertainty of the charge measurement ( $\approx 5\%$ ) was not considered in the errors computation.

Another problem was the pedestal position: the zero-peak was very different (almost hundred counts) for few PMTs, due to unknown reason. With the exception of the PMT SA0207, that shows a baseline shift during the same run (at 850 V), the pedestal shift was not impeding the gain and single photoelectron resolution measurements.

#### SA0164 -- Pixel single ph.el. resolution

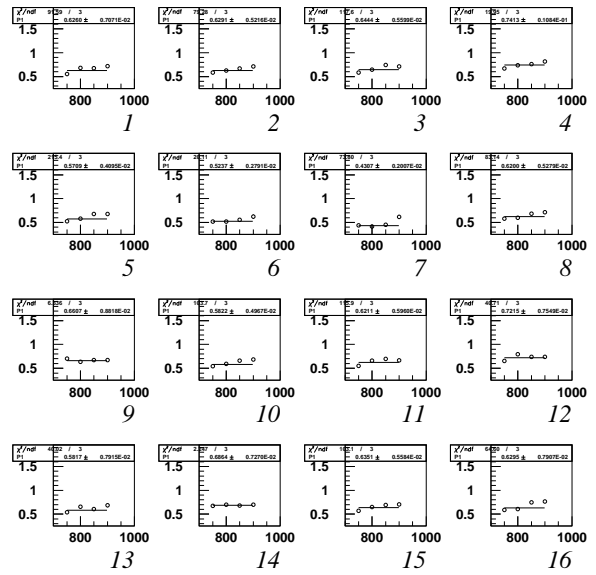


**Figure 7.** Single photoelectron resolution as function of the HV value, measured in Grenoble.

##### 4.2. Results

The single photoelectron resolution is relatively insensitive to the HV settings and sometimes is better at low voltage (figure 7), while with the Bologna setup has sometimes the opposite behavior (figure 8).

There are large fluctuations between adjacent ADC channels (even if the statistics are high enough: 63'000 events), probably due to the “sample and hold” technique. The systematic bin-wise fluctuations are negligible after rebinning: the ADC has an effective 10 bits resolution (figure 9).

The last produced PMTs show a more uniform behavior than the first ones: the Hamamatsu production chain “stabilized” around PMT SA0190 (see figure 10). This can be important when selecting the PMTs for the final detector.

#### 5. PMT selection criteria

##### 5.1. Expected dynamic range

The 16 channels ADC is perfectly linear over its full scale (4096 counts) and has two gain scales (a factor of 5 in dynamic range), but the preamplifier OPA 340 reduces the linear range to 2/3 of the full-scale. A test of an improved version of the chip is foreseen on

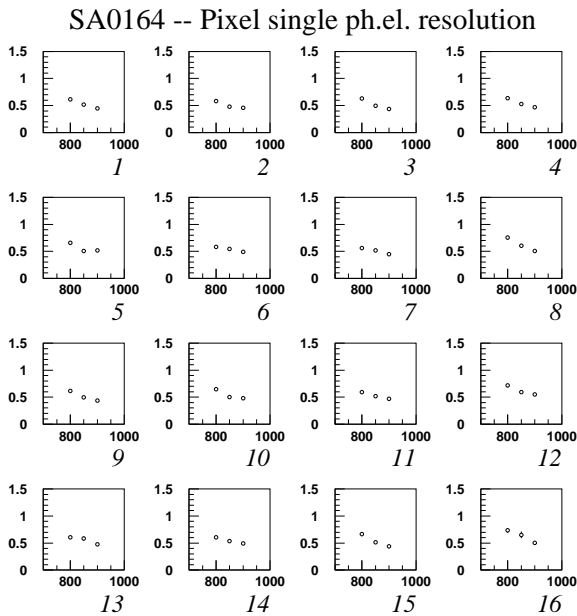


**Figure 8.** Single photoelectron resolution as function of the HV value, measured in Bologna.

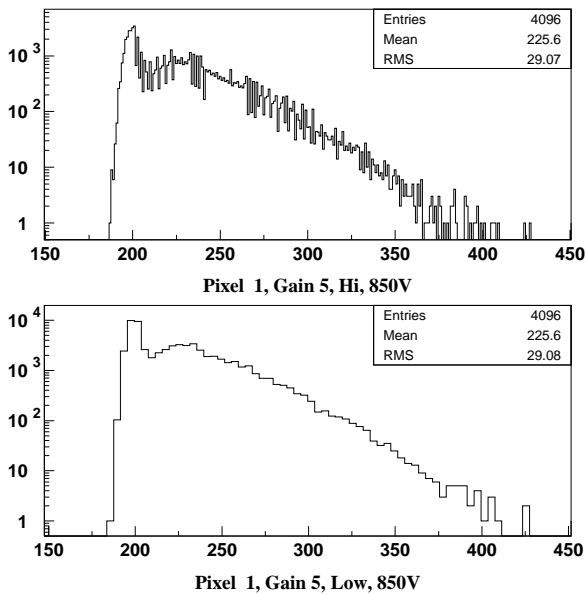


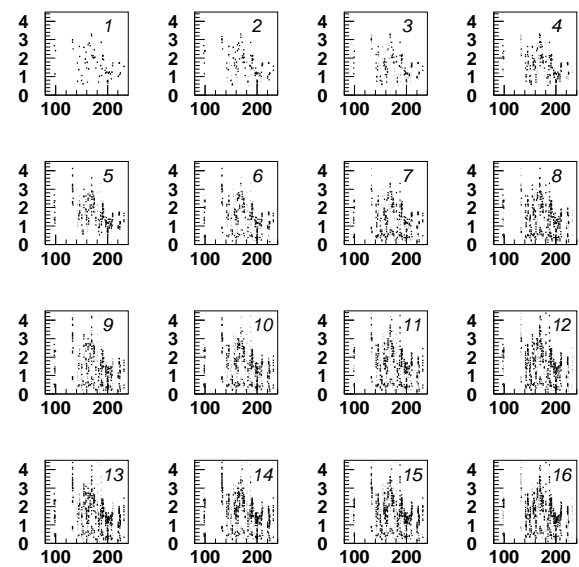
**Figure 9.** The effective resolution of the AD7476ART ADC chip is 10 bits.

September 2001<sup>3</sup>.

The front-end electronics will read each pixel over

<sup>3</sup>J. Pouxe, private communication.

Pixel gain/ $10^6$  VS. PMT number, at 850V



*Calibrations done at ISN, Grenoble*

**Figure 10.** All pixels gain distribution for  $V = 850V$ , measured in Grenoble.

threshold, asking the ADC for the  $5\times$  scale if not saturated or else the  $1\times$  scale. We will assume that the  $5\times$  scale is perfectly linear. If the pedestal position is before the 500 ADC counts, we can consider at least 3500 ADC counts as the effective linear dynamic range in the  $5\times$  scale.

The simulated mean number of photoelectrons per pixel produced by a Fe nucleus is about 20, but their distribution has a tail reaching approximately 100 phel/pixel<sup>4</sup>.

If we set the voltage in order to have 50 (10) counts in the  $5\times$  ( $1\times$ ) scale for the single photoelectron peak, we will be able to reach 70 phel/pixel counts in the  $5\times$  scale, i.e. the linear range reaches the Fe nuclei.

## 5.2. HV settings

The plot of the tension  $V^*$  needed to have 50 ADC counts in the  $5\times$  scale corresponding to 1 phel/pixel (figure 11) shows that all the PMTs tested in Grenoble (with the exception of SA0132, SA0152, SA0168, SA0169, SA0187) need a voltage in the range  $-(780 \div 880)V$ , that is not very large. In addition, there is a sharp indication that the last produced PMTs (from

<sup>4</sup>J. Casaus, private communication.

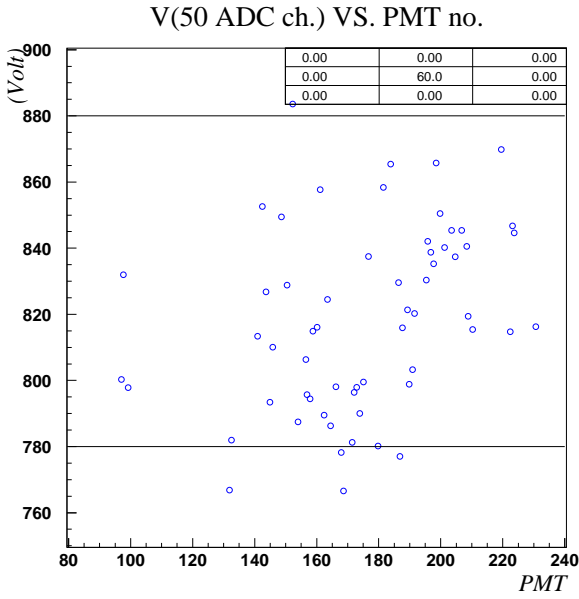


**Figure 11.** Distribution of the voltage  $V^*$  needed to have on the average 50 ADC counts for the single photoelectron peak in the  $5 \times$  scale.

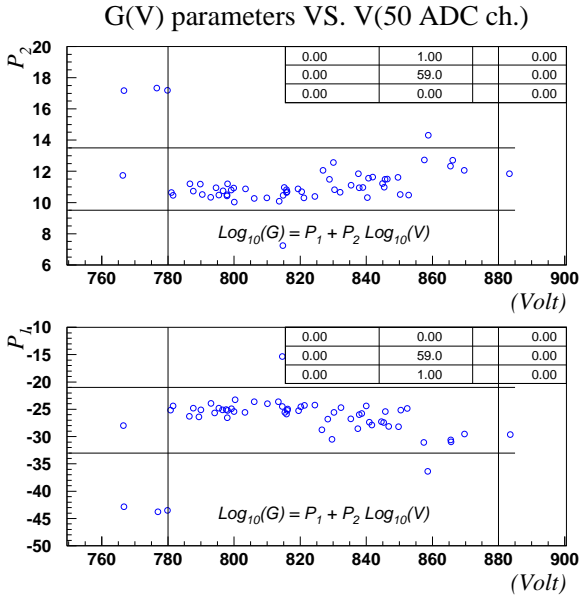


**Figure 12.** Distribution of the gain to voltage fit parameters as function of  $V^*$ .

SA0190 on) are grouped in a narrower range, as effect of the stabilized production chain.

The PMTs installed in the final detector will be powered in small sets (5 or 6 PMTs per HV channel),

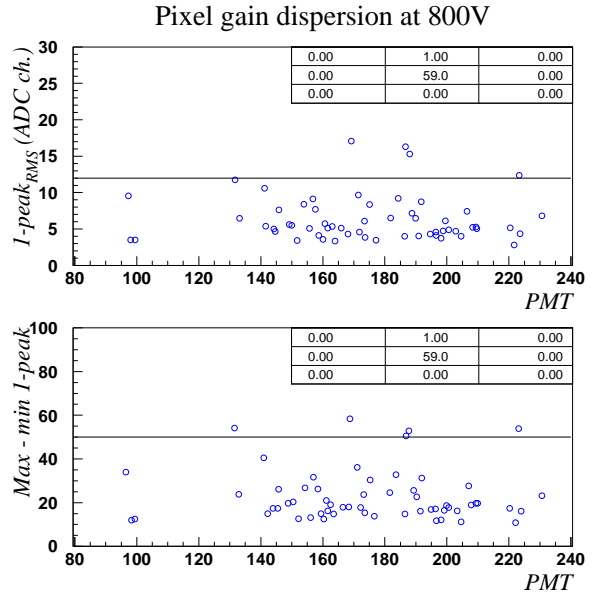


**Figure 13.** Distribution of the RMS 1-peak to 0-peak distance (up) and maximum distance difference (down), in ADC counts.

connected as daisy-chains. In addition to  $V^*$ , these sets should have similar gain to voltage dependence, in order to guarantee a good collective behavior in case of small adjustments of the tension.

The plot of the fit parameters (see eq. 2) shows that other 3 PMTs (SA0159, SA0180, SA0182) should be discarded, due to very different values from the rest of the sample (accepted ranges:  $-33 < P_1 < -21$  and  $9.5 < P_2 < 13.5$ ).

In total, 8 PMTs over 60 show bad values, and they have serial numbers lower than 190.

### 5.3. Pixel gain and efficiency

The values plotted in figures 11 and 12 are mean values, but we have also to consider the pixel related quantities. For example we should choose PMTs with a little spreading between pixel gains. This can be done by looking at the position of the 1-peak with respect to the 0-peak, as in figure 13.

If we ask that the RMS dispersion be less than 12 ADC counts and the maximum difference be less than 50 ADC counts, two additional PMTs are rejected (SA0188 and SA0223). Noticeable is that SA0223 is the first PMT after SA0190 that doesn't satisfy the requirements.

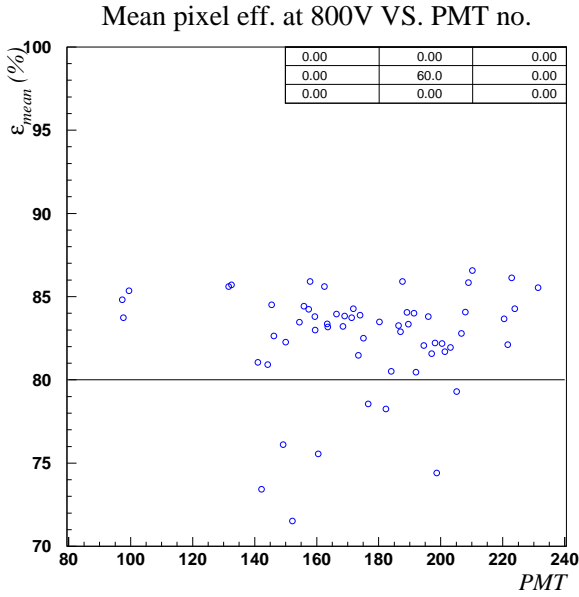


**Figure 14.** Distribution of the mean pixel efficiency.

The last things we can look into are the mean pixel efficiency and the efficiency spreading per PMT. In order to have a definition of the (relative) pixel efficiency that can be used for all the PMTs, we adopted the following definition:

$$\varepsilon \equiv \frac{N - N_0}{N_0} \quad (4)$$

where  $N = 63'000$  is the DAQ triggers number and  $N_0$  is the normalization constant of the Gaussian fit to the 0-peak. Assuming that the geometry and the LED behavior don't change appreciably between different runs,  $N_0$  is roughly the inefficiency of the pixel.

The bad news here are that even though the efficiency shows a little convergence increasing the serial number, the fluctuations are large: the mechanical construction does stabilize, but the material of the photocathode does not.

Referring to figures 14 and 15, we chose 80% as lowest value for the mean efficiency, 8% and 35% as highest thresholds on the RMS efficiency and maximum difference, respectively. The results are (already discarded PMTs are not shown):

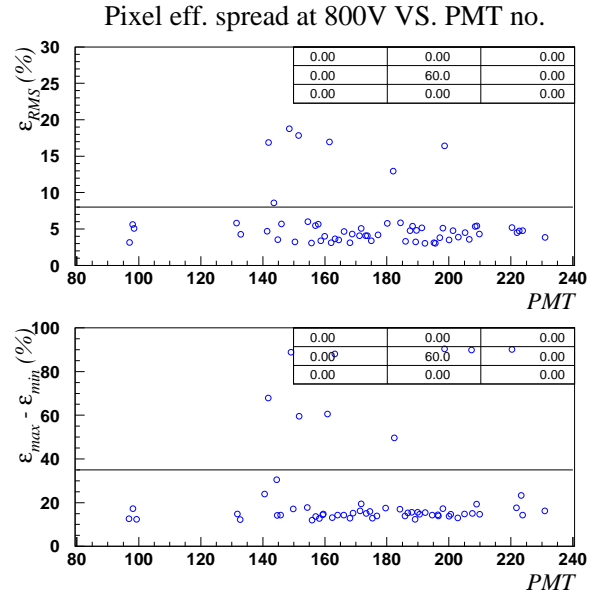


**Figure 15.** Spreading of the pixel efficiencies.

PMT	$\langle \varepsilon \rangle$ (%)	$\varepsilon_{\text{RMS}}$ (%)	$\varepsilon_{\text{max}} - \varepsilon_{\text{min}}$ (%)
<b>SA0142</b>	73.89	17.40	67.03
<b>SA0149</b>	76.84	18.30	88.45
<b>SA0161</b>	75.43	17.77	61.90
SA0163	83.67	4.37	89.58
SA0177	78.02	3.83	12.21
<b>SA0199</b>	74.58	16.41	90.44
SA0205	79.53	4.50	14.58
SA0207	82.67	4.31	88.57
SA0220	83.06	4.96	91.57

where boldface PMT names match all three negative conditions.

A summary table for all the 60 PMTs tested in Grenoble is given in the Appendix.

In conclusion, a very high number of PMTs is rejected using all the suggested cuts. Even though the stabilization of the production chain is very promising for what concerns the gain behavior (and we could hope to discard no PMT due to bad voltage or fit parameters), it is unlikely that much less than the present fraction of 10% (18% using the OR of conditions on efficiencies) of PMTs will not be discarded due to bad pixel efficiencies when selecting the 740 ones to be mounted in the final assembly.

**Appendix: Test results with ISN setup**

PMT	$V^*$ (Volt)	$P_1$	$P_2$	$d_{\text{RMS}}$ (ADC counts)	$d_{\text{max}} - d_{\text{min}}$	$\langle \varepsilon \rangle$ (%)	$\varepsilon_{\text{RMS}}$ (%)	$\varepsilon_{\text{max}} - \varepsilon_{\text{min}}$ (%)
SA0097	800.5	-23.03	10.02	9.422	33.90	84.74	4.219	13.99
SA0098	832.4	-24.99	10.63	3.585	11.50	83.16	4.891	17.76
SA0099	797.7	-24.45	10.51	3.503	12.60	85.12	4.539	14.00
SA0132	766.4	-27.87	11.76	11.93	54.90	85.25	4.572	15.11
SA0133	781.8	-24.05	10.41	6.390	23.10	85.77	4.389	13.78
SA0141	813.8	-23.60	10.19	10.73	40.17	81.57	5.903	22.23
SA0142	852.7	-25.01	10.60	5.107	14.80	73.89	17.40	67.03
SA0144	826.6	-29.04	12.03	4.802	17.28	81.00	7.628	30.12
SA0145	793.1	-23.69	10.26	4.654	17.77	84.19	4.372	14.18
SA0146	810.0	-23.89	10.30	7.537	26.52	82.55	4.513	14.52
SA0149	849.5	-27.99	11.62	5.555	19.40	76.84	18.30	88.45
SA0150	828.3	-27.37	11.46	5.463	20.68	82.26	4.365	16.80
SA0152	883.2	-29.23	11.98	3.418	12.80	71.35	17.61	58.34
SA0154	787.5	-25.12	10.76	8.147	26.00	83.25	4.775	16.81
SA0156	806.2	-23.68	10.23	4.936	13.80	84.29	4.482	13.86
SA0157	795.8	-24.65	10.58	9.040	31.19	84.81	4.507	13.25
SA0158	794.6	-25.60	10.91	7.651	26.58	85.09	4.590	13.92
SA0159	815.0	-15.21	7.307	3.950	14.60	83.74	4.474	15.17
SA0160	816.2	-25.54	10.85	3.440	12.60	82.45	4.474	14.34
SA0161	857.2	-31.10	12.67	5.850	21.00	75.43	17.77	61.90
SA0162	789.4	-26.29	11.17	5.246	16.38	85.10	4.142	12.98
SA0163	824.5	-24.25	10.39	5.327	19.50	83.67	4.365	89.58
SA0164	786.2	-26.31	11.18	3.565	14.10	83.64	4.463	14.03
SA0166	798.2	-26.38	11.18	5.346	17.50	83.79	4.504	15.69
SA0168	778.1	-97.29	35.75	4.348	17.00	83.54	4.110	13.21
SA0169	766.7	-43.42	17.15	17.09	58.96	83.05	4.390	14.89
SA0171	781.2	-25.11	10.78	9.883	36.35	83.36	4.284	16.32
SA0172	797.0	-24.92	10.68	4.591	17.09	84.95	5.255	19.25
SA0173	798.2	-24.64	10.58	6.152	23.20	81.38	4.042	14.78
SA0174	789.9	-24.65	10.60	3.638	15.10	83.39	4.281	15.37
SA0175	799.5	-25.65	10.92	8.293	30.84	82.65	4.225	13.63
SA0177	837.5	-28.93	11.97	3.377	13.90	78.02	3.832	12.21
SA0180	780.0	-43.42	17.11	88.20	355.2	83.85	4.633	16.98
SA0182	858.6	-35.87	14.29	6.334	24.00	78.55	12.05	49.36
SA0184	865.0	-30.04	12.29	9.223	32.50	80.69	4.739	16.68
SA0186	829.9	-30.45	12.51	3.972	14.20	83.41	4.070	13.39
SA0187	776.7	-44.10	17.35	16.46	50.60	82.21	5.136	14.75
SA0188	816.0	-25.05	10.68	15.23	52.40	85.97	4.968	15.76
SA0189	821.3	-24.13	10.36	7.133	25.30	84.07	3.977	13.20
SA0190	799.3	-24.84	10.65	6.532	22.53	83.04	4.600	15.46
SA0191	803.5	-25.65	10.91	4.154	16.00	84.06	4.518	15.48
SA0192	819.9	-25.04	10.67	8.717	31.60	80.97	4.427	14.40

---

SA0195	830.3	-25.84	10.93	4.313	16.06	82.26	4.438	14.35
SA0196	841.8	-28.19	11.71	4.551	17.40	83.60	4.445	15.30
SA0197	838.7	-25.53	10.80	4.110	11.90	81.16	4.279	13.10
SA0198	835.0	-26.49	11.14	3.632	12.22	82.13	4.863	16.65
SA0199	865.6	-31.53	12.80	4.627	17.00	74.58	16.41	90.44
SA0200	850.2	-24.75	10.52	6.030	18.91	82.12	4.473	13.62
SA0201	839.8	-24.01	10.28	4.858	17.48	81.10	4.640	15.30
SA0203	845.5	-25.94	10.93	4.546	16.40	81.17	4.175	13.22
SA0205	837.6	-25.64	10.84	4.024	11.78	79.53	4.504	14.58
SA0207	845.7	-27.53	11.48	7.223	27.84	82.67	4.314	88.57
SA0208	840.3	-27.47	11.47	5.358	18.70	84.25	4.752	15.91
SA0209	819.6	-25.89	10.97	5.275	19.86	85.66	5.401	19.67
SA0210	815.1	-25.56	10.86	5.073	19.10	86.12	4.311	15.27
SA0220	869.4	-29.29	12.03	5.128	17.10	83.06	4.961	91.57
SA0222	815.1	-24.75	10.58	2.826	10.41	82.63	4.766	16.35
SA0223	846.9	-27.64	11.51	12.54	53.20	86.53	5.819	22.68
SA0224	844.9	-27.06	11.31	4.330	16.00	84.07	4.542	15.67
SA0231	816.3	-25.06	10.69	6.779	23.90	85.84	4.491	16.17

---